Acta Cryst. (1972). A28, 607

Vacancy Short-Range Order in Substoichiometric Transition Metal Carbides and Nitrides with the NaCl Structure. II. Numerical Calculation of Vacancy Arrangement

BY M. SAUVAGE* AND E. PARTHÉ

Laboratoire de Cristallographie aux Rayons X, Université de Genève, Geneva, Switzerland

(*Received* 12 *May* 1972)

Using Babinet's theorem and certain results of the theory of short-range order originally developed for Cu_3Au alloys it is shown that the diffuse scattering intensity in the electron diffraction patterns of the substoichiometric transition metal carbides is related to a short-range order of carbon vacancies. Numerical values for the short-range order parameters can be obtained by integrating over the total diffuse intensity within one repetitive unit in reciprocal space. To perform such calculations on $VC_{0.75}$ an analytical function was identified which describes the shape of the diffuse intensity curves in reciprocal space. Making the simplifying assumption that the value of the diffuse intensity is 1 on the diffuse intensity curve and 0 everywhere else numerical values for the vacancy short-range order in $VC_{0.75}$ were obtained. The results, represented as average numbers of vacancies in different coordination shells around a vacancy, agree with the general principles of vacancy arrangement found in ordered transition metal carbides and nitrides.

Introduction

As has been shown in detail in Part I of the present paper, (Billingham, Bell & Lewis, 1972), transition metals of groups IV and V with carbon and nitrogen form substoichiometric compounds with the NaCl structure type exhibiting vacancy short-range order within certain domains of composition and temperature. It is commonly assumed that the f.c.c. partial structure of the metal atoms is perfect while vacancies occur in the carbon or nitrogen f.c.c. partial structure: one is then dealing with a short-range order problem in a 'binary compound' $A_{xA}B_{xB}$ where A denotes here a vacancy and B a carbon or nitrogen atom. Such problems have already been treated in the case of metallic phases: Au–Cu alloys (Cowley, 1950; Moss, 1964) or Au–Pd alloys (Lin, Spruiell & Williams, 1970).

As is well known, short-range order in direct space will result in non-zero diffuse scattering between the nodes of the mean reciprocal lattice. According to Cowley's theory (Warren, 1969), the analysis of this diffuse intensity, measured by X-ray or electron diffraction techniques, enables one to derive the most probable local arrangement for A and B atoms in the compound.

The purpose of the present work is to apply Cowley's theory, which we will treat in the first section, to carbides and nitrides of transition metals with the NaCl structure type. The experimental material for the diffuse intensity measurements are the electron diffraction patterns presented in Fig. 2 of Part I. The calculations are made for the particular compound $VC_{0.75}$, but our results can be easily extended to other compounds and compositions.

Information on the local vacancy arrangement in these compounds is of particular interest since the latter is directly related to the nature of bonding between the metal and the non-metal atoms (Lye, 1971; Nowotny & Neckel, 1969).

Correlation between diffuse intensity and short-range order parameters

The most general expression for the amplitude scattered by a vanadium carbide single crystal grain is:

$$R(\mathbf{H}') = \sum_{j}^{\substack{\text{all V atoms in}\\ \text{single crystal}}} f_V \exp(2\pi i\, \mathbf{H}' \cdot \mathbf{r}_{V_j}) + \sum_{i}^{\substack{\text{all C atoms in}\\ \text{single crystal}}} f_C \exp(2\pi i \mathbf{H}' \cdot \mathbf{r}_{C_i}) \quad (1)$$

where $\mathbf{H}'$ denotes a vector in reciprocal space with continuously varying coordinates.

One gets a more useful expression for the amplitude of a scattered beam, in a vacancy type carbide, by adding and subtracting the contribution of carbon atoms which are actually missing in the real object.

$$R(\mathbf{H}') = \sum_{j}^{\substack{\text{all V atoms in}\\ \text{single crystal}}} [f_V \exp(2\pi i \mathbf{H}' \cdot \mathbf{r}_{V_j}) + f_C \exp\{2\pi i \mathbf{H}' \cdot (\mathbf{r}_{V_j} + \mathbf{a}/2)\}] - \sum_{g}^{\substack{\text{vacancy sites in}\\ \text{single crystal}}} f_C \exp(2\pi i \mathbf{H}' \cdot \mathbf{r}_{\square_g}) \quad (2)$$

where $\mathbf{a}$ is one translation vector of the direct cubic lattice.

The first summation gives the amplitude scattered by a perfectly stoichiometric VC single crystal grain with NaCl structure. As is well known, this summation

* On leave from the Laboratoire de Minéralogie-Cristallographie associé au C.N.R.S., Université de Paris VI, France.

equals zero for any $\mathbf{H}'$ vector different from $\mathbf{H}=h\mathbf{a}^*+k\mathbf{b}^*+l\mathbf{c}^*$ where h, k, l are integers all odd or all even. Introducing the number N of cubic unit cells in the object one obtains:

$$R(\mathbf{H}')=\begin{cases}\pm N.4(f_V\pm f_C)-\sum\limits_{g}^{\text{vacancy sites in single crystal}} f_C\exp(2\pi i\mathbf{H}'.\mathbf{r}_{\square_g}) \\ \text{when } \mathbf{H}'=\mathbf{H} \qquad (3a)\\ -\sum\limits_{g}^{\text{vacancy sites in single crystal}} f_C\exp(2\pi i\mathbf{H}'.\mathbf{r}_{\square_g}) \qquad (3b)\\ \text{when } \mathbf{H}'\neq\mathbf{H}\ .\end{cases}$$

From now on, only the intensities or amplitudes scattered in directions $\mathbf{H}'$ different from $\mathbf{H}$, *i.e.* in between the mean reciprocal lattice points corresponding to a real f.c.c. lattice, will be considered. The expression (3*b*) for the amplitude $R(\mathbf{H}')$ appears as a summation over the *vacant* carbon sites in the single crystal grain. If we now imagine an 'atom', denoted by the symbol $\square$, having a scattering factor $f_\square$ equal to zero, located on every site actually occupied by a carbon atom in the single crystal, we are able to write the amplitude $R(\mathbf{H}')$ as a summation over all possible carbon sites in the single crystal grain:

$$R(\mathbf{H}')=-\left\{\sum_{g}^{\text{vacancy sites in single crystal}} f_C\exp(2\pi i\mathbf{H}'.\mathbf{r}_{\square_g})+\sum_{i}^{\substack{\text{actually occupied carbon atom sites}\\ \text{in single crystal}}} f_\square\exp(2\pi i\mathbf{H}'.\mathbf{r}_{Ci})\right\}$$

$$=-\sum_{j}^{\text{all possible carbon sites in single crystal}} f_{Mj}\exp(2\pi i\mathbf{H}'.\mathbf{r}_{Mj})$$

where $f_{Mj}=f_C$ or $f_\square$. (4)

Considering the NaCl structure, one can see that $R(\mathbf{H}')$ describes the amplitude scattered by a distribution of carbon atoms and vacancies on all the sites of a single crystal with an $A1$ (Cu) structure type. However, this distribution is *complementary* to the actual distribution and corresponds to the average composition $\square_{0.75}C_{0.25}$, the actual composition being $VC_{0.75}\square_{0.25}$. This result is a direct consequence of Babinet's theorem on complementary screens in diffraction theory.

Our problem, concerning short-range order in the ‚binary compound', $\square_{0.75}C_{0.25}$, is then closely related to the similar problem of the binary alloy Cu_3Au, already studied by Cowley (1950) and which is thoroughly treated in Warren's (1969) book.

In what follows, we will make extensive use of Warren's notation, as far as it is suitable for our problem.

The diffuse intensity due to short-range order, in directions $\mathbf{H}'$, different from $\mathbf{H}$, is given by:

$$I_{SRO}(\mathbf{H}')=R(\mathbf{H}').R(\mathbf{H}')^*=\sum_{j}^{A1}\sum_{j'}^{A1} f_{Mj}.f_{Mj'}\exp\{(2\pi i\mathbf{H}'.(\mathbf{r}_{Mj}-\mathbf{r}_{Mj'})\} \quad (5)$$

where $A1$ is used here as a simplified notation for the sentence 'all possible sites in a single crystal with $A1$ structure type'.

The mean value for the product $f_{Mj}.f_{Mj'}$ is:

$$\langle f_M f_{M'}\rangle=(0{\cdot}75f_\square+0{\cdot}25f_C)^2=0{\cdot}0625f_C^2\,. \quad (6)$$

Adding and subtracting this mean value, one obtains for $I_{SRO}(\mathbf{H}')$:

$$I_{SRO}(\mathbf{H}')=\sum_{j}^{A1}\sum_{j'}^{A1}(f_{Mj}.f_{Mj'}-0{\cdot}0625f_C^2)\exp\{2\pi i\mathbf{H}'.(\mathbf{r}_{Mj}-\mathbf{r}_{Mj'})\}+0{\cdot}0625f_C^2\sum_{j}^{A1}\sum_{j'}^{A1}\exp\{2\pi i\mathbf{H}'.(\mathbf{r}_{Mj}-\mathbf{r}_{Mj'})\}\,. \quad (7)$$

The second summation has values different from zero only if $\mathbf{H}'=\mathbf{H}$. However since we are interested only in vectors $\mathbf{H}'\neq\mathbf{H}$ this summation can be omitted from the further development of the theory.

The first summation is made of pairs such as:

$$(f_{Mj}.f_{Mj'}-0{\cdot}0625f_C^2)\exp\{2\pi i\mathbf{H}'.(\mathbf{r}_{Mj}-\mathbf{r}_{Mj'})\}+(f_{Mj'}.f_{Mj}-0{\cdot}0625f_C^2)\exp\{2\pi i\mathbf{H}'.(\mathbf{r}_{Mj'}-\mathbf{r}_{Mj})\}$$

it can then be written as a cosine sum:

$$I_{SRO}(\mathbf{H}')=\sum_{j}^{A1}\sum_{j'}^{A1}(f_{Mj}.f_{Mj'}-0{\cdot}0625f_C^2)\times\cos 2\pi\mathbf{H}'.(\mathbf{r}_{Mj}-\mathbf{r}_{Mj'})\,. \quad (8)$$

As there is only one atom per Bravais lattice point in the $A1$ structure, any vector $\mathbf{r}_n=(\mathbf{r}_{Mj}-\mathbf{r}_{Mj'})$ must be a lattice translation as well. Let us consider all pairs of atoms in the object which are separated by such a vector $\mathbf{r}_n$ and we will denote by $\langle f_M f_{M'}\rangle_n$ the mean value of $f_M f_{M'}$, for all those pairs and by Z_n their number. Using these new quantities the expression for $I_{SRO}(\mathbf{H}')$ can be written as a simple summation:

$$I_{SRO}(\mathbf{H}')\simeq\sum_{n=0}^{\substack{\text{all vectors connecting a given carbon site to other possible carbon sites in a single crystal with } A1 \text{ structure}}} Z_n(\langle f_M f_{M'}\rangle_n-0{\cdot}0625f_C^2)\cos 2\pi\mathbf{H}'.\mathbf{r}_n\,. \quad (9)$$

To simplify the notation, we will use from now on the symbol VEC($A1$) to represent the set of vectors over which the summation is to be performed.

In short-range ordered structures the mean value $\langle f_M f_{M'}\rangle_n$ is different from the general mean value $\langle f_M f_{M'}\rangle=0{\cdot}0625f_C^2$ only for short vectors $\mathbf{r}_n$. In this case the number Z_n can be approximated by the number of carbon sites in the single crystal which is $4N$, N being the number of cubic unit cells, and then:

$$I_{SRO}(\mathbf{H}') \simeq \sum_{n=0}^{VEC(A1)} 4N(\langle f_M f_{M'} \rangle_n - 0{\cdot}0625 f_C^2) \times \cos 2\pi \mathbf{H}' \cdot \mathbf{r}_n \,. \quad (10)$$

Following Warren's treatment, we will introduce two probabilities, valid for the complementary structure $\square_{0.75}C_{0.25}$:

$p_\square(n)$: probability of finding a vacancy $\square$ as a $\mathbf{r}_n$ neighbour of a carbon atom,

$p_C(n)$: probability of finding a carbon atom as a $\mathbf{r}_n$ neigbour of a vacancy.

Let $x_\square$ and x_C be the concentrations of vacancies and carbon atoms respectively in the complementary structure. The number of pairs $\square C$ separated by a particular vector $\mathbf{r}_n$ is then given by $p_C(n) \cdot x_\square \cdot 4N$. Obviously this is equal to the number of pairs $C\square$ separated by the opposite vector $-\mathbf{r}_n$ which is $p_\square(-n) \cdot x_C \cdot 4N$. Assuming that the distribution of vacancies is statistically centrosymmetrical that means $p_\square(n) = p_\square(-n)$, one obtains the following general equation

$$x_\square p_C(n) = x_C p_\square(n) \,. \quad (11)$$

When carbon atoms and vacancies are randomly distributed one gets, in addition, the relations

$$p_C(n) = x_C \quad \text{and} \quad p_\square(n) = x_\square \,. \quad (12a)$$

In the case of a preference for *unlike* $\mathbf{r}_n$ neighbours, one finds:

$$p_C(n) > x_C \quad \text{and} \quad p_\square(n) > x_\square \,. \quad (12b)$$

The contrary holds in the case of a preference for $\mathbf{r}_n$ neighbours of the same kind:

$$p_C(n) < x_C \quad \text{and} \quad p_\square(n) < x_\square \,. \quad (12c)$$

Using $p_\square(n)$ and $p_C(n)$ the expression for $\langle f_M f_{M'} \rangle_n$ is:

$$\begin{aligned} \langle f_M f_{M'} \rangle_n &= x_C f_C [p_\square(n) f_\square + (1 - p_\square(n)) f_C] \\ &\quad + x_\square f_\square \{ p_C(n) f_C + [1 - p_C(n)] f_\square \} \\ &= x_C f_C^2 [1 - p_\square(n)] \end{aligned} \quad (13)$$

$$\begin{aligned} \langle f_M f_{M'} \rangle_n - \langle f_M f_{M'} \rangle^{\text{random distribution}} &= x_C f_C^2 [1 - p_\square(n)] - x_C^2 f_C^2 \\ &= x_C x_\square f_C^2 \left[1 - \frac{p_\square(n)}{x_\square} \right] \\ &= 0{\cdot}1875 f_C^2 \left[1 - \frac{p_\square(n)}{x_\square} \right] . \end{aligned} \quad (14)$$

Introducing Cowley's short-range order parameters $\alpha(n)$ given by: *

$$\alpha(n) = 1 - \frac{p_\square(n)}{x_\square} = 1 - \frac{p_C(n)}{x_C} \,, \quad (15)$$

* In a recent review article by Cowley (1971) the parameter is called 'Warren order parameter'.

one obtains for $I_{SRO}(\mathbf{H}')$:

$$I_{SRO}(\mathbf{H}') \simeq 0{\cdot}75 N f_C^2 \sum_{n=0}^{VEC(A1)} \alpha(n) \cos 2\pi \mathbf{H}' \cdot \mathbf{r}_n \,. \quad (16)$$

The physical meaning of $\alpha(n)$ is very simple:

random distribution	$\alpha(n) = 0$
preference for unlike $\mathbf{r}_n$ neighbour	$\alpha(n) < 0$
preference for like $\mathbf{r}_n$ neighbour	$\alpha(n) > 0$.

When $\mathbf{r}_n$ becomes large, $\alpha(n)$ tends toward zero as there is no longer any correlation between the occupation of the two sites separated by $\mathbf{r}_n$.

In the $A1$ structure type, any interatomic vector can be expressed as:

$$\mathbf{r}_n = l \frac{\mathbf{a}_1}{2} + m \frac{\mathbf{a}_2}{2} + n \frac{\mathbf{a}_3}{2} \,, \quad (17)$$

$\mathbf{a}_1$, $\mathbf{a}_2$, $\mathbf{a}_3$ being the three translation vectors of the cubic unit cell and l, m, n being *integers whose sum is even.*

On the other hand $\mathbf{H}'$ can be written as:

$$\mathbf{H}' = h_1 \mathbf{a}_1^* + h_2 \mathbf{a}_2^* + h_3 \mathbf{a}_3^* \,, \quad (18)$$

$\mathbf{a}_1^*$, $\mathbf{a}_2^*$, $\mathbf{a}_3^*$ being the corresponding reciprocal lattice vectors and h_1, h_2, h_3 *continuously varying coordinates* in reciprocal space. Writing $\alpha(lmn)$ for $\alpha(n)$, equation (16) becomes:

$$I_{SRO}(h_1 h_2 h_3) \simeq 0{\cdot}75 N f_C^2 \sum_{l=-\infty}^{+\infty} \sum_{m=-\infty}^{+\infty} \sum_{n=-\infty}^{+\infty} \alpha(lmn) \times \cos \pi (h_1 l + h_2 m + h_3 n) \quad (19)$$

with $l+m+n$ even.

Although the single crystal is only of limited size, we have used for the summation limits $+\infty$ and $-\infty$. This is possible as the values of $\alpha(lmn)$ tend to zero for large l, m or n. It is further assumed that the vacancy distribution on possible carbon sites is statistically symmetrical and thus

$$\alpha(lmn) = \alpha(\pm l \pm m \pm n) \,. \quad (20)$$

When expanding $\cos \pi(h_1 l + h_2 m + h_3 n)$ as a sum of triple products of trigonometric functions and gathering terms corresponding to the values $+l+m+n$, $-l+m+n$, $+l-m+n$, $+l+m-n$ one can easily check that all terms but the *cosine* triple product disappear. Then:

$$I_{SRO}(h_1 h_2 h_3) \simeq 0{\cdot}75 N f_C^2 \sum_{l=-\infty}^{+\infty} \sum_{m=-\infty}^{+\infty} \sum_{n=-\infty}^{+\infty} \alpha(lmn) \times \cos \pi l h_1 \cos \pi m h_2 \cos \pi n h_3 \,. \quad (21)$$

Formula (21) shows that the diffuse intensity is periodic in reciprocal space with the periods $\Delta h_1 = 2$, $\Delta h_2 = 2$, and $\Delta h_3 = 2$ along the directions $\mathbf{a}_1^*$, $\mathbf{a}_2^*$, $\mathbf{a}_3^*$ of the reciprocal lattice fundamental translations.

Standard Fourier inversion techniques give for $\alpha(lmn)$ the following expression:

$$\alpha(lmn) \simeq \frac{1}{0{\cdot}75\,.\,Nf_C^2\,.\,8} \int_{h1=-1}^{+1} \int_{h2=-1}^{+1} \int_{h3=-1}^{+1} I_{SRO}\,(h_1h_2h_3) \cos \pi l h_1 \cos \pi m h_2 \cos \pi n h_3 \, \mathrm{d}h_1 \mathrm{d}h_2 \mathrm{d}h_3 \,. \quad (22)$$

The set of parameters $\alpha(lmn)$ is defined only when l, m and n are integers the sum of which is even. Later on it will be shown that $I_{SRO}(h_1h_2h_3)$ has cubic symmetry. As a consequence α takes the same value for directions which are equivalent according to cubic symmetry:

$$\alpha(lmn) = \alpha(lmn\circlearrowleft) = \alpha(lnm\circlearrowleft) \,. \quad (23)$$

The $\alpha(lmn)$ parameter is very simply related to the occupation of the coordination shell specified by lmn. Let $n_{max}(lmn)$, $n_C(lmn)$ and $n_\square(lmn)$ denote the total number of sites, the number occupied by carbon atoms and the number occupied by vacancies respectively. If, for example, it is assumed that a vacancy is situated at the origin one obtains for the real structure where $x_C = 0{\cdot}75$:

$$n_C(lmn) = n_{max}(lmn) x_C [1 - \alpha(lmn)]$$
$$n_\square(lmn) = n_{max}(lmn) - n_C(lmn) \,. \quad (24)$$

Knowing the intensity distribution $I_{SRO}(h_1h_2h_3)$ one is able to obtain by use of formulae (22) and (24) the most probable distribution of vacancies in the single crystal.

For compositions other than $VC_{0.75}$ the numerical factor in equation (22) will be different. However, as later calculations show, the α values can be normalized independently.

Evaluation of experimental diffuse intensity data for $VC_{0.75}$

Evaluation of equation (22) requires that diffuse intensity data be measured over the whole repeating volume of reciprocal space. Two difficulties are encountered here:

(*a*) Only a limited number of planar sections through the repeating volume are available,

(*b*) Intensity measurements on electron diffraction patterns cannot be very accurate.

For the solution of the first problem one may make use of symmetry considerations. The reciprocal lattice corresponding to a face-centered cubic structure is invariant to the symmetry operations of space group $Im3m(O_h^9)$. The diffuse intensity in reciprocal space exhibits the same symmetry. As a proof one may study the 9 electron diffraction patterns shown in Fig. 2 of Part I and their two-dimensional space groups given in Table 1. The symmetry elements found agree with those one should recognize in planes passing through the origin of a periodic object with space group $Im3m$. In order to construct a three-dimensional model of the diffuse intensity one can thus use the intensity data from one electron diffraction pattern for all the symmetry related planes. For example the [001] photograph can be used for 6 sections of the repeating unit (3 cube faces and 3 middle planes of the cube sides).

Table 1. *Two-dimensional space groups of different electron diffraction patterns*

Type of plane normal (u, v, w without common factor)		Two dimensional space group of diffuse scattering pattern	Examples
[00w]		$p4m$	[001]
[0vv]		cmm	[011]
[uuu]		$p6m$	[111]
[0vw]	$v+w=2n+1$	pmm	[012], [014], [023]
	$v+w=2n$	cmm	[013], [015], [035]
[uuw]	$2u+w=2n+1$	cmm	[113], [115], [221], [223], [443]
	$2u+w=4n+2$	cmm	[114], [118], [334]
	$2u+w=4n$	pmm	[112], [116], [332]
[uvw]		$p2$	[123], [124], [125]

By using the data from four major electron diffraction patterns (001, 011, 111 and 112) it was possible, to construct a three-dimensional model of the diffuse intensity in reciprocal space shown in Fig. 1. The shape of this model is strikingly similar to the shape of the theoretical Fermi surface of a primitive cubic metal having one electron per atom [Fig. 2 after Sommerfeld & Bethe (1933)].

The second difficulty concerns the actual value of the diffuse intensity. A study of the electron diffraction patterns in Fig. 2 of Part I indicates that the diffuse intensity has nearly the same value all over the diffuse bands. To simplify the evaluation we have assumed the constant value of 1 for $I_{SRO}(h_1h_2h_3)$ on the diffuse bands and the value 0 everywhere else. As equation

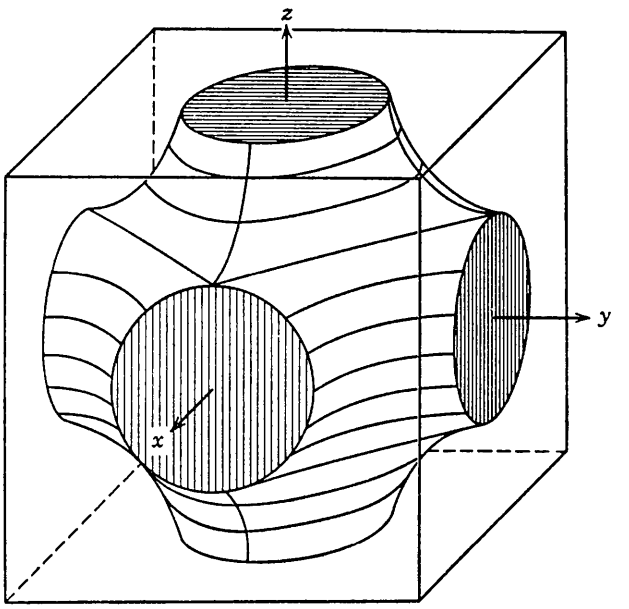

Fig. 2. Possible, constant-energy surface for a simple cubic metal after Sommerfeld & Bethe (1933).

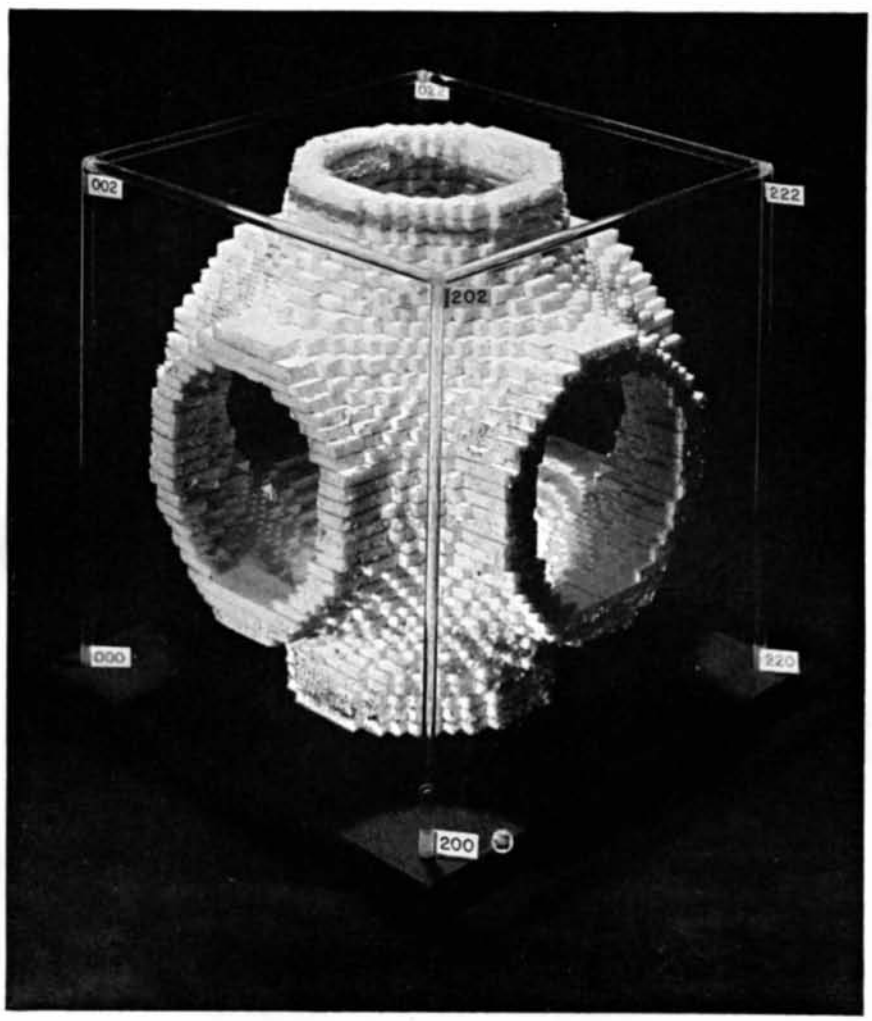

Fig. 1. Model of diffuse intensity in reciprocal space.

[*To face p.* 610

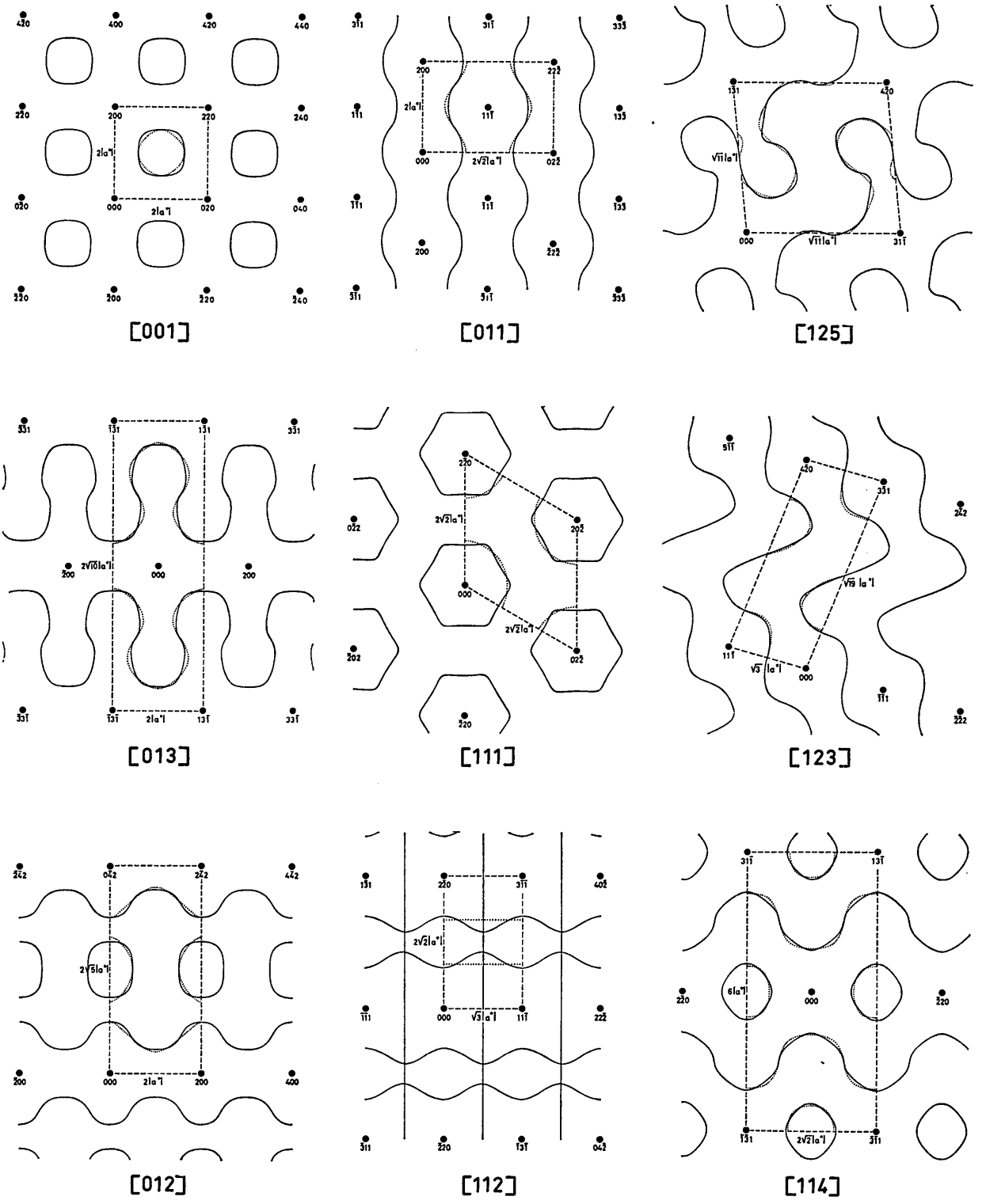

Fig. 3. Nine sections through the diffuse intensity surface calculated with equation (28*a*) (dotted lines) and (28*b*) (full lines). In [112] the straight vertical lines occur in both cases independently of the C_{111} value.

(22) can be normalized independently it is not necessary here to determine the absolute value of $I_{SRO}(h_1h_2h_3)$.

Analytical formulation of the shape of the diffuse intensity in reciprocal space

We have emphasized above that the shape of the diffuse intensity shows a striking resemblance to the theoretical Fermi surface of a simple cubic metal. For an analytical expression of this shape we can thus use the mathematical expressions developed for the Fermi surfaces.

The distribution of the diffuse intensity is triply periodic with periods $\Delta h_1=2$, $\Delta h_2=2$ and $\Delta h_3=2$ and can be described by a function of the type

$$\sum_{pqr} C_{pqr} f_{pqr}(h_1h_2h_3)=0 \qquad (25)$$

where the sum $p+q+r$ is *an odd integer*, C_{pqr} is a constant and $f_{pqr}(h_1h_2h_3)$ has the general formulation:

$$f_{pqr}(h_1h_2h_3)=\begin{cases}\cos^p \pi h_1 \,.\, \cos^q \pi h_2 \,.\, \cos^r \pi h_3 \\ +\cos^p \pi h_2 \,.\, \cos^q \pi h_3 \,.\, \cos^r \pi h_1 \\ +\cos^p \pi h_3 \,.\, \cos^q \pi h_1 \,.\, \cos^r \pi h_2 \\ +\cos^p \pi h_2 \,.\, \cos^q \pi h_1 \,.\, \cos^r \pi h_3 \\ +\cos^p \pi h_1 \,.\, \cos^q \pi h_3 \,.\, \cos^r \pi h_2 \\ +\cos^p \pi h_3 \,.\, \cos^q \pi h_2 \,.\, \cos^r \pi h_1 \,. \end{cases} \qquad (26)$$

To match the diffuse intensity surfaces with good accuracy only one or two terms of (25) are needed depending on the sample and composition. Although the shapes of the diffuse intensities for all the different compounds given in Figs. 2 and 4 of Part I are essentially identical, there are small differences. As an example one may compare the [001] diffuse intensity patterns of $VC_{0.75}$, (Part I, Fig. 2) and $NbC_{0.7}$ (Part I, Fig. 4): the 'circles' in $NbC_{0.7}$ are more 'square' shaped in $VC_{0.75}$.

We found that all the different, slightly varying, diffuse intensity surfaces fall within two limiting surfaces described by equation (25) with the following constants:

(*a*) $C_{100}=1$, $C_{111}=0$ and all other $C_{pqr}=0$ (27*a*)

(*b*) $C_{100}=1$, $C_{111}=-1$ and all other $C_{pqr}=0$. (27*b*)

As

$$f_{100}(h_1h_2h_3)=2\,(\cos \pi h_1+\cos \pi h_2+\cos \pi h_3)$$

and

$$f_{111}(h_1h_2h_3)=6\,(\cos \pi h_1 \,.\, \cos \pi h_2 \,.\, \cos \pi h_3)$$

the two limiting analytical functions are given by;

(*a*) $\cos \pi h_1+\cos \pi h_2+\cos \pi h_3=0$ (28*a*)

(*b*) $\cos \pi h_1+\cos \pi h_2+\cos \pi h_3 - 3(\cos \pi h_1 \,.\, \cos \pi h_2 \,.\, \cos \pi h_3)=0$. (28*b*)

Fig. 3 shows a set of 9 sections through the surface calculated from equation (28*b*) (with $C_{111}=-1$) which matches the set of 9 electron diffraction patterns of Fig. 2 in Part I. The agreement is quite satisfactory even for very aslant sections such as [123] or [125]. Within the marked unit cells the surface described by equation (28*a*) with $C_{111}=0$ is indicated by dotted lines.

As mentioned above, the C_{111} value seems to depend on the compound under investigation and, for each particular compound, on its composition and thermal history. The C_{111} value can be measured conveniently by the position of the intersection of the diffuse inten-

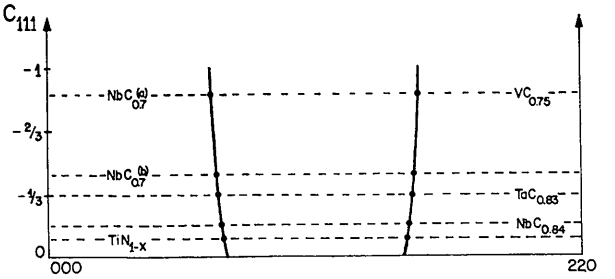

Fig. 4. Intersection of diffuse intensity surfaces with the vector connecting the origin to the reciprocal lattice point 220, as a function of C_{111}. The experimentally measured C_{111} values of the different compounds are only approximate and correspond to the centre of the diffuse band. If the spacing between the 000 and 220 spots is denoted by $D_{(000-220)}$ and the distance between the two diffuse bands in between by D_{diff}, the value of C_{111} is given by:

$$C_{111}=-\frac{1+2\cos 2\pi F}{3\cos^2 2\pi F} \text{ with } F=\tfrac{1}{2}\frac{D_{(000-220)}-D_{diff}}{D_{(000-220)}}\,.$$

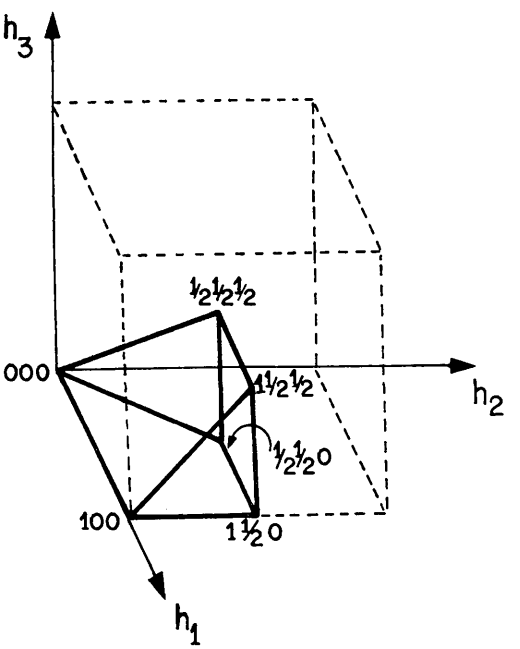

Fig. 5. Minimum volume needed for numerical integration, corresponding to $\frac{1}{96}$ of the unit cell in reciprocal space (translation periods $\Delta h_1=2$, $\Delta h_2=2$, $\Delta h_3=2$).

sity surface with the vector joining the origin with the reciprocal lattice point 220. In Fig. 4 is shown the change in position of these intersection points as a function of C_{111} together with experimentally determined C_{111} values for four compounds.

As the 220, or any symmetry-related reciprocal-lattice point occurs on many diffraction patterns (*e.g.* [001], [011], [111], [112] and [114]) several measurements of C_{111} have been made for each compound. In the case of $VC_{0.75}$ the values are all in good agreement

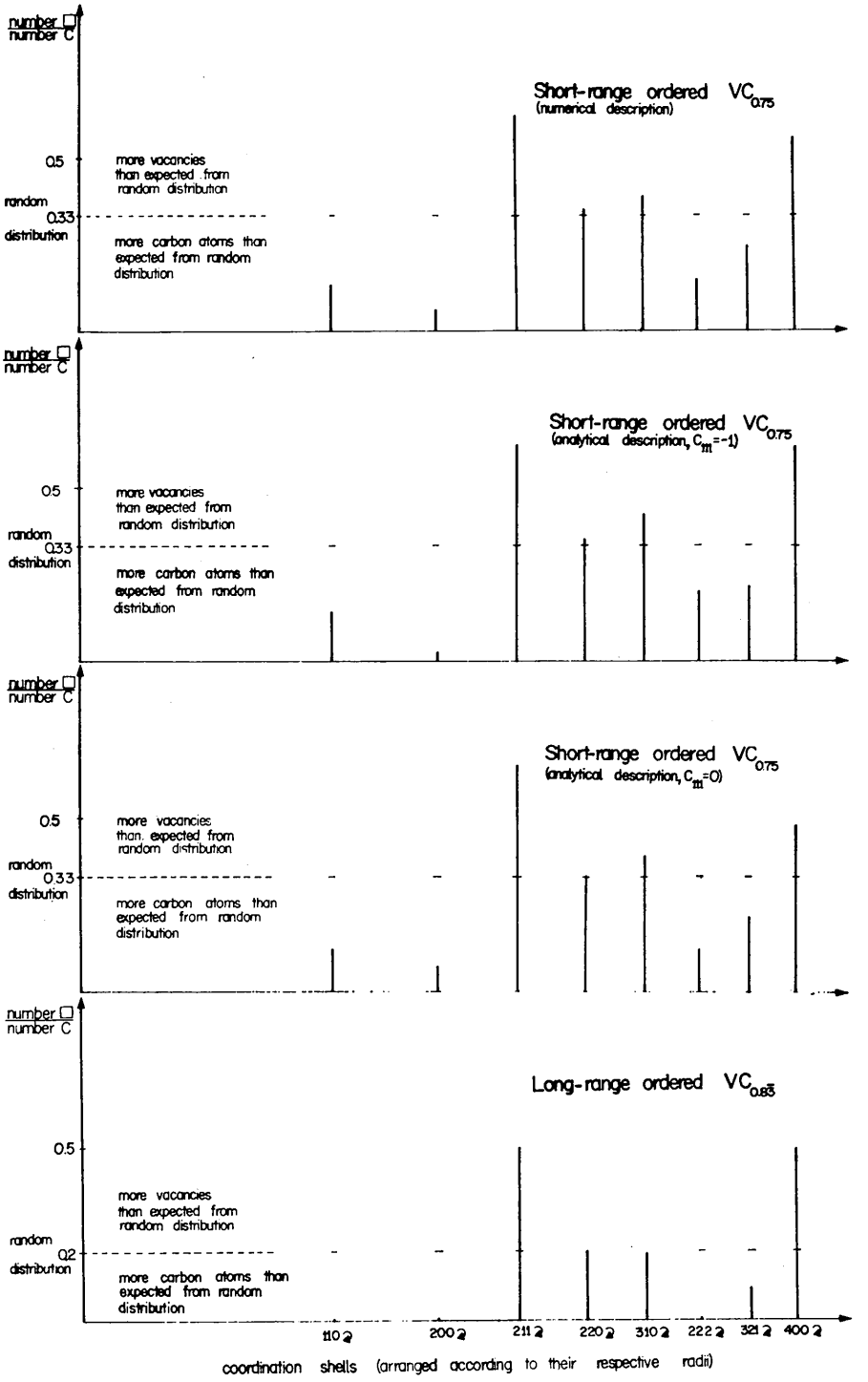

Fig. 6. $n_{\square}/n_C$ values for short-range ordered vanadium carbide and long-range ordered V_6C_5 ($\equiv VC_{0.83}$).

with a C_{111} value about $-\frac{5}{6}$ whereas for $NbC_{0.7}$ the measurements performed on the [011] pattern ($NbC_{0.7}$ (*a*) on Fig. 4) and on the [001] pattern ($NbC_{0.7}$ (*b*) on Fig. 4) differ. The [011] and [001] diffraction patterns were recorded from thin sections of the same polycrystalline sample of nominal composition $NbC_{0.7}$. The discrepancy may be due either to localized fluctuations in carbon concentration or to modifications in the local vacancy order following different cooling rates from the heat-treatment temperature.

Measurements have also been performed on electron diffraction patterns of the two carbides $NbC_{0.84}$ and $TaC_{0.83}$ (Venables & Meyerhoff, 1971, quoted in part I). One can see that as the composition approaches M_6C_5 the C_{111} value tends towards zero. For the long-range ordered phase M_6C_5, superstructure reflexions are actually observed along the 220 reciprocal lattice row at the same positions where the diffuse intensity surface, corresponding to $C_{111}=0$, intersects.

For the case of the nitride TiN_{1-x}, two determinations of C_{111} ([011] and [111] patterns of Fig. 4, Part I) are consistent with a very small value. Indeed, the diffuse intensity curves in the [111] pattern are very close to circles as is to be expected for $C_{111}=0$ (Fig. 3).

Calculation of vacancy short-range order in vanadium carbide

The calculation of the short-range order parameters $\alpha(lmn)$ could be carried out analytically if it were only possible to perform the integration in the expression:

$$\alpha(lmn) \sim \int\int_0^2\int \delta[\sum_{pqr} C_{pqr} f_{pqr}(h_1h_2h_3)] \times \cos \pi l h_1 \,.\, \cos \pi m h_2 \,.\, \cos \pi n h_3 dh_1 dh_2 dh_3 \,. \quad (29)$$

The Dirac δ function has been introduced to provide a value of 1 everywhere on the diffuse intensity surface and zero elsewhere. In our evaluation we have replaced the integral by numerical summations. The $\alpha(lmn)$ were calculated by two procedures.

(1) No analytical function was used to describe the diffuse intensity surface.

The repeating volume in reciprocal space had been divided in $40\times40\times40$ elementary cubes (intervals of 0·05 for h_1, h_2 and h_3). Each of these elementary cubes was assigned a coefficient 1 or 0 according to whether, from a study of Fig. 1, it contained diffuse intensity or not.

By taking into account the invariance of the diffuse intensity surface with respect to the symmetry operations of the space group $Im3m(O_h^9)$, it was sufficient to consider only those points located in 1/96 of the repeating volume and to give each point a weight corresponding to its proper multiplicity factor (96 for a general position, 48, 24, 12 or even 8 for more symmetrical positions).

The small volume over which we performed the summation is shown on Fig. 5.

The expression for $\alpha(lmn)$ becomes then:

$$\alpha(lmn) = K \sum_{h1=0}^{1} \sum_{\substack{h2=0 \\ h2\le h1}}^{\pm} \sum_{\substack{h3=0 \\ h3\le h2}}^{\pm} g(h_1h_2h_3) I_{SRO}(h_1h_2h_3)$$
$$\times \{\cos \pi l h_1 \cos \pi m h_2 \cos \pi n h_3 + \cos \pi l h_2 \cos \pi m h_3 \cos \pi n h_1 + \cos \pi l h_3 \cos \pi m h_1 \cos \pi n h_2 + \cos \pi l h_2 \cos \pi m h_1 \cos \pi n h_3 + \cos \pi l h_1 \cos \pi m h_3 \cos \pi n h_2 + \cos \pi l h_3 \cos \pi m h_2 \cos \pi n h_1\} \quad (30)$$

where $g(h_1h_2h_3)$ is proportional to the multiplicity factor,

$$I_{SRO}(h_1h_2h_3) \text{ is 0 or 1}$$

and K is determined by the normalization condition: $\alpha(000)=1$.

The values of $\alpha(lmn)$ for the first eight coordination shells, obtained with this procedure, are listed in the second column of Table 2. The number of points involved in the calculation is 9716. It has been checked that small changes in the model chosen for the diffuse intensity distribution had but little influence on the $\alpha(lmn)$ values.

Table 2. *Values of $\alpha(lmn)$ calculated for short-range ordered vanadium carbide with different descriptions of I_{SRO} and the long-range ordered phase V_6C_5*

	$\alpha(lmn)$			
	Numerical description	Analytical description of I_{SRO}		Long-range ordered phase
lmn	of I_{SRO}	$C_{111}=-1$	$C_{111}=0$	V_6C_5
110	−0·178	−0·171	−0·190	−0·200
200	−0·260	−0·300	−0·241	−0·200
211	+0·176	+0·176	+0·190	+0·200
220	+0·008	+0·011	+0·006	0
310	+0·041	+0·064	+0·046	0
222	−0·171	−0·109	−0·184	−0·200
321	−0·070	−0·099	−0·100	−0·100
400	+0·143	+0·179	+0·056	+0·200

(2) The analytical description of the diffuse intensity surface is used to select the points involved in the summation.

The h_1h_2 plane is scanned with steps of 0·01 for h_1 and h_2, h_3 being calculated through equations (28*a*) or (28*b*) for each couple h_1 h_2 leading to a real solution. A summation similar to equation (30) is then performed over the set of points h_1 h_2 h_3 determined in this way. In the third and forth columns of Table 2 are given the first eight $\alpha(lmn)$ values calculated for the two limiting cases corresponding to $C_{111}=-1$ (45596 data points) and $C_{111}=0$ (51226 data points).

For comparison, $\alpha(lmn)$ values calculated for the long-range ordered phase $VC_{0.83}$ are listed in the fifth column of Table 2. One can see that the $\alpha(lmn)$ obtained by following procedures 1 and 2 are similar to

Table 3. *Occupation of different coordination shells surrounding a vacancy in short-range ordered* $VC_{0.75}$ *and long-range ordered* V_6C_5 ($\equiv VC_{0.83}$)

		Numerical I_{SRO}		Analytical I_{SRO} $C_{111}=-1$		Analytical I_{SRO} $C_{111}=0$		Long-range ordered V_6C_5	
lmn	n_{max} (*lmn*)	n_C (*lmn*)	$n_\square$(*lmn*)	n_C (*lmn*)	$n_\square$(*lmn*)	n_C (*lmn*)	$n_\square$(*lmn*)	n_C (*lmn*)	$n_\square$(*lmn*)
110	12	10·6	1·4	10·5	1·5	10·7	1·3	12	0
200	6	5·65	0·35	5·85	0·15	5·6	0·4	6	0
211	24	14·8	9·2	14·8	9·2	14·5	9·5	16	8
220	12	8·9	3·1	8·9	3·1	9	3	10	2
310	24	17·3	6·7	16·9	7·1	17·2	6·8	20	4
222	8	7	1	6·65	1·35	7·1	0·9	8	0
321	48	38·5	9·5	39·5	8·5	39·5	8·5	44	4
400	6	3·85	2·15	3·7	2·3	4·2	1·8	4	2

one another and not very different from the values calculated for the long-range ordered structure.

Using the experimentally determined $\alpha(lmn)$ values one is able to derive, by use of equations (24), the most probable local arrangement of vacancies.

The values of $n_C(lmn)$ and $n_\square(lmn)$ are listed in Table 3. The ratio $n_\square/n_C$ for successive coordination shells is plotted in Fig. 6 for the short-range ordered phase $VC_{0.75}$ and long-range ordered $V_6C_5(VC_{0.83})$. There is a striking similarity between the two diagrams which can be interpreted in the following way.

Due to the existence of a repulsion between vacancies the number of vacancies in the first two coordination shells around a vacancy is as small as possible:

– for $VC_{0.83}$ (long-range ordered) this number is *zero* for the first two shells, the vacancies being concentrated in the third shell 211.

– for $VC_{0.75}$ there is a larger number of vacancies in the structure and some must be located in the 110 and 200 shells but their number is very small and much lower than expected from a random distribution. Most of the vacancies are in the third shell as in the long-range ordered case.

As pointed out in Part I, theories have been proposed to explain why this long-range ordered arrangement, where each vanadium (or niobium) atom is surrounded by 5 carbon atoms and 1 vacancy, is particularly stable (Lye, 1971). Although this theory is not accepted by all groups working on the band structure of transition metal compounds, it is quite striking that the most probable local distribution in the short-range ordered compounds reproduces similar surrounding for vanadium atoms. This result is in good agreement with the n.m.r. data of Froidevaux & Rossier (1967).

As shown above, for all compounds discussed one finds to a rough approximation the same diffuse intensity surface. Since the values of $\alpha(lmn)$ do not depend on concentration, all these compounds will thus have approximately similar $\alpha(lmn)$ values which, at least for the first eight shells, are not so very different from those calculated for the long-range ordered phase M_6C_5. The essential difference in the most probable vacancy arrangement is, according to equation (24), simply controlled by the actual composition. As a consequence, for example in short-range ordered $TaC_{0.84}$ the most probable local arrangement is the same as in long-range ordered M_6C_5. This result is quite different from that observed in the short-range ordered metallic alloys and is probably a consequence of the more directional character of bonding.

Conclusion

By use of an analytical description of the diffuse intensity surface, it has been possible to derive the type of short-range order encountered in the cubic carbides VC_{1-x}, NbC_{1-x}, TaC_{1-x} and nitride TiN_{1-x}.

This work could be developed in two main directions. Firstly it would be interesting to determine the factors needed to describe the exact shape of the diffuse intensity surface (characterized by the value of the constant C_{111}).

Secondly, the diffuse scattering could be used to obtain information on the Fermi surface of the compounds investigated. Such work has already been performed by Castles, Cowley & Spargo (1971) for titanium oxide (see also Cowley, 1969). We are presently carrying out a similar study on vanadium carbide, using the energy band calculations made by Neckel, Rastl, Weinberger & Mechtler (1972); let us just mention here that the Fermi surface of VC is very similar to the Fermi surface of TiN (Ern & Switendick, 1965). This is to be expected as both compounds give similar diffuse scattering in their short-range ordered state. Further results in this field will be published in a later paper.

We would like to express our thanks to Professor Lacroix who has drawn our attention to the similarity between the diffuse intensity and the Fermi surface of a simple cubic metal, which enabled us to find the proper analytical description. We also wish to thank Professor M. Peter for very helpful discussions.

References

BILLINGHAM, J., BELL, P. S. & LEWIS, M. H. (1972). *Acta Cryst.* A**28**, 602.

CASTLES, J. R., COWLEY, J. M. & SPARGO, A. E. C. (1971). *Acta Cryst.* A**27**, 376.

COWLEY, J. M. (1950). *J. Appl. Phys.* **21**, 24.

COWLEY, J. M. (1969). *The Chemistry of Extended Defects in Non-metallic Solids*, edited by L. EYRING and M. O'KEEFE, p. 259. Amsterdam: North Holland.
COWLEY, J. M. (1971). *Advanc. High Temp. Chem.* **3**, 35.
ERN, V. & SWITENDICK, A. C. (1965). *Phys. Rev.* **137**A, 1927.
FROIDEVAUX, C., & ROSSIER, D. (1967). *J. Phys. Chem. Solids*, **28**, 1197.
LIN, W., SPRUIELL, J. E. & WILLIAMS, R. O. (1970). *J. Appl. Cryst.* 3, 297.
LYE, R. G. (1971). RIAS Technical Report 71–21c.
MOSS, S. C. (1964). *J. Appl. Phys.* **35**, 3547.
NECKEL, A., RASTL, P., WEINBERGER, P. & MECHTLER, R. (1972). *Theor. Chim. Acta (Berlin)*, **24**, 170.
NOWOTNY, H. & NECKEL, A. (1969). *J. Inst. Metals*, **97**, 161.
SOMMERFELD, A. & BETHE, H. (1933). *Handbuch der Physik* **24**/2. second ed., p. 400. Berlin: Springer.
VENABLES, J. D. & MEYERHOFF, M. H. (1971). NBS Symposium on Novel High Temperature Materials, Gaithersburg, Md. (Proceedings to be published in 1972).
WARREN, B. E. (1969). *X-ray Diffraction*, p.p 227, 232 ff. Reading: Addison–Wesley.

Acta Cryst. (1972). A**28**, 616

A Lattice-Dynamical Treatment of the Thermal-Motion Bond-Length Correction

BY C. SCHERINGER

Institut für Kristallographie der Universität, Karlsruhe, Germany

(*Received* 4 *July* 1972)

The effect of the thermal motions of the atoms on interatomic distances is treated in terms of lattice dynamics. It is not only shown how the anisotropic vibration tensors of the atoms can be derived from the dynamical matrices of the crystal but also how mean binary-product coupling tensors are obtained. Each of these tensors expresses the coupling of the motions of two atoms in the unit cell as an average over time and lattice and thus is suitable for formulating the bond-length correction. Hence the discussion centres around the coupling tensors. The coupling tensors cannot be determined by experiment; but in order to calculate them and the bond-length correction, one is forced to conceive dynamical models of motion for the atoms in the unit cell. The corrections for the known models of uncorrelated motion, rigid-body motion and riding motion are rederived by using the coupling tensors.

1. Introduction

The effect of the thermal motions of the atoms on interatomic distances has been discussed by Cruickshank (1956, 1961), Busing & Levy (1957, 1964), Schomaker & Trueblood (1968), and Johnson (1970). Structure refinement with X-ray and/or neutron data provides the mean positions of the atoms in the unit cell. The distance between the mean positions of the atoms is generally considered as a good approximation of the 'true' distance between the atoms. It is, however, more exact to define the 'true' distance to be the time and lattice average of all instantaneous distances, whereby this distance is usually larger because the atoms usually do not vibrate in phase in the planes perpendicular to the distance vector. Diffraction methods applied to crystals do not provide any phase relationships for the motions of neighbouring atoms. Hence one is forced to conceive dynamical models of motion for which the phase relationships are defined. These allow one to calculate the bond-length correction. The models, which have been used in the past, are the models of rigid-body motion, riding motion, and uncorrelated motion.

Two methods have been applied to derive the bond-length correction from a given dynamical model. Cruickshank (1956, 1961) investigated how rigid-body motion effects the electron-density distribution of the atoms in question. The calculation of the correction is based on determining the correct positions of the electron-density maxima which represent the atoms. As a new concept Busing & Levy (1957, 1964) introduced the joint distribution of the atoms in question and thus defined the 'true' distance as the average over the joint distribution of the two atoms. The actual calculation of the correction is thus based on the solution of convolution integrals. The concept of the joint distribution also plays the prominent part in Johnson's (1970) review.

Our approach to determining the correction will be derived from a lattice-dynamical investigation of the anisotropic vibration tensors. A central concept in describing the dynamics of a crystal is the dynamical matrices. In a preceding paper (Scheringer, 1972) we showed how the anisotropic vibration tensors can be expressed by way of the dynamical matrices of the crystal. In a similar manner one can also obtain mean binary-product coupling tensors. Each of these tensors expresses the coupling of the motions of two atoms in the unit cell as an average over time and lattice and thus contains the respective phase relationships. Hence the coupling tensors are suitable for formulating the bond-length correction, and in this paper our discussion will centre around them.

Unfortunately, the coupling tensors cannot be deter-